COMSOL
CONFERENCE
2026 SHENZHEN

Numerical Analysis of Swirl Formation and Turbulence Modelling in Local Dry Welding Chamber

Ganta Venkateswara Rao[1], Milan Kumar Maity[1], Saurav Suman[1]
1. Department of Mechanical Engineering, National Institute of Technology Mizoram, Aizawl, India, 796012.

Abstract
Underwater local dry welding (ULDW) is a prominent method for performing marine joints and repairs, whereas local dry-welding chambers require a stable flow of drainage gas to prevent water ingress and hydrogen diffusion, thereby ensuring weld quality. In this study, a stationary computational fluid dynamics (CFD) investigation was conducted to analyze the flow behavior within a novel conical local dry-welding chamber with an angled inlet configuration. To evaluate the influence of velocity and inlet geometry (8mm radius) on swirl formation, turbulence development, pressure distribution, and flow stabilization. Air was used as the working fluid, with an inlet velocity of 45 m/s, a constant outlet pressure of 0 Pa, an inlet radius of 8 mm, and an outlet radius of 20 mm. A physics-dependent fine mesh is applied to the chamber to assess the flow regime and numerical accuracy. A Three-dimensional (3D) model was developed in COMSOL Multiphysics® version 6.3, using the CFD module and the Shear Stress Transport (SST) turbulence model, coupled with the Reynolds Average Navier Stokes (RANS) model under stationary conditions. The study included evaluations of velocity magnitude, pressure contours, axial velocity, and swirl number (S), which were extracted using COMSOL's post-processing. The swirl number decreased significantly from 7.6601 at the inlet to 1.1664 at the outlet, with an average of 4.4903. The axial velocity decreases from top to bottom as the chamber length decreases. The results showed that it generated a stronger vortex flow field, with a large pressure drop at the outlet due to the velocity effect. This work shows the usefulness of COMSOL Multiphysics® for the CFD analysis and optimization of underwater welding systems. The methodology can be extended to other shielding gas chambers, jet-driven devices, and vortex-based industrial flow applications.
Keywords: ULDW, local dry welding chamber, CFD, vortex, swirling flow

Introduction
Underwater welding (UWW) is the method used for marine joints and offshore repairs. It was primarily divided into 2 types, wet and dry welding, based on the way it was done. ULDW is another method that evolved from wet and dry welding. It is the method used to create a dry environment at the welding site[1]. In UWW, the surrounding water makes it more challenging than conventional atmospheric welding. Water surrounding the welding site may affect arc stability, heat transfer, weld formation, and the welding environment [2]. Therefore, creating the controlled gaseous region around the welding site is important.

ULDW is a promising method for protecting weld formation and joint quality. It will create the localized gaseous region around the welding site. A local dry welding chamber drives around the weld region, and gas is supplied through the chamber to displace the water [3], [4]. The resulting dry region allows welding to be performed in a more controlled gaseous environment. However, simply supplying the drainage gas through the chamber will not guarantee a stable, dry cavity. The gas must effectively displace the water ingress by giving a covering around the weld region. The adequate pressure field must be maintained by avoiding excessive recirculation [5].

Strong velocity gradients, vortex formation, recirculation, swirling flow, and spatial pressure changes are all part of the intrinsically three-dimensional internal flow produced by several tangential inlets. It is difficult to directly experimentally characterize these variables inside the restricted chamber, especially in the vortex core and inlet interaction region. The underlying flow structure may thus be resolved, and the spatial development of velocity, pressure, turbulence, vorticity, and swirl can be quantified using three-dimensional CFD.

In this study, we designed a three-dimensional (3D) ULDW chamber. The welding chamber is a device comprising cylindrical and conical bodies with 4 tangential inlets and 1 outlet, which serves as an underflow for gas drainage and has a hole for the welding torch. In the present work, COMSOL Multiphysics® 6.3 is employed to develop a three-dimensional stationary RANS model using theSST turbulence model. The simulation is used to characterize the velocity field, pressure distribution,

streamline structure, swirling flow, and axial evolution of the swirl number within the conical local dry welding chamber.

Numerical Methodology

The numerical methodology was established in two subsections: mathematical modeling and geometric details, and governing equations and their source terms, as follows.

Mathematical modeling & Geometry details

A three-dimensional computational model of the underwater local dry-welding chamber was developed in COMSOL Multiphysics® 6.3, as shown in Figure 1. The chamber consists of a cylindrical upper section connected to a conical skirt, with four symmetrically arranged angled and tangential gas inlets to generate swirling flow. A central opening is provided for the welding torch, while the lower opening serves as the gas outlet [6] . The tangential arrangement of the inlet ports introduces circumferential momentum into the chamber, resulting in a three-dimensional swirling flow field [7] .

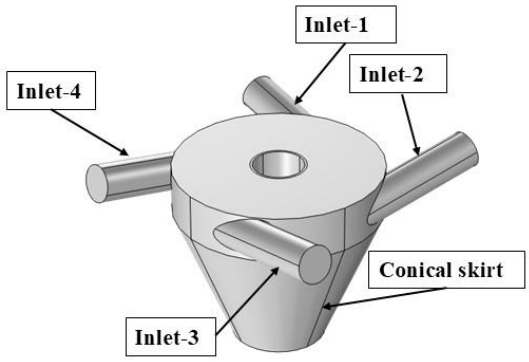


Figure 1. Isometric view Underwater local dry welding chamber designed in COMSOL

The inlet and outlet radii were taken as 8 mm (for all 4 inlets) and 20mm. Velocity is taken as 45 m/s at the inlet, and pressure is taken as 0 Pa at the outlet. The gas flow was modeled as three-dimensional, incompressible, turbulent, and stationary. Air was considered the working fluid with constant thermophysical properties. The chamber walls were treated as stationary no-slip boundaries. The flow was solved using the RANS formulation with the SST turbulence model [8], [9] .

Governing Equations and Basis Terms

A single-phase turbulent SST model was implemented in COMSOL. Since the model uses the air as a working fluid and is considered incompressible, the continuity Eq. (1 is governed as

$$\Delta . u = 0 \tag{1}$$

where u is the mean velocity vector.

The conservation of momentum Eq. (2) is governed as

$$\rho(u.\nabla)u = -\nabla p + \nabla \cdot [(\mu + \mu_t)(\nabla u + (\nabla u)^T)] \tag{2}$$

Where ρ is the fluid density, u is the velocity, p is the pressure, μ is the dynamic viscosity, and μ_t is the turbulent viscosity. Turbulent momentum transport was represented using the SST $k-\omega$ turbulence model.

The mathematical quantity of velocity components in the swirling formation is governed by Eq. (3)

$$U = \sqrt{u_r^2 + u_\theta^2 + u_Z^2} \tag{3}$$

Where u_r is the radial velocity, and u_θ is the tangential velocity, and u_z is axial velocity.

The swirl number quantifies the strength of rotational flow relative to axial flow. The general definition is Eq. (4)

$$S = \frac{G_\Theta}{RG_Z} \tag{4}$$

Where G_Θ is the axial flux of angular momentum, G_z is the axial flux of axial momentum, R is the characteristic chamber outlet radius. The reported equation in integral form is Eq.(5)

$$S = \frac{\int_A \rho V_z V_\theta \, r dA}{R \int_A \rho V_z^2 \, dA} \tag{5}$$

Where, V_z is axial velocity, V_θ is tangential velocity, r is the radial coordinate, A is the chamber cross-sectional area. The swirl number was calculated on multiple cross-sectional planes along the chamber axis to quantify the spatial evolution of angular momentum and vortex intensity [10] .

A physics-controlled mesh was generated in COMSOL Multiphysics® 6.3 to adequately resolve the high velocity gradients near the inlet regions, chamber walls, and outlet. Three mesh levels, coarse, normal, and fine, were investigated to assess mesh sensitivity. The predicted flow characteristics (swirl number) were compared across different mesh levels to assess the sensitivity of the numerical solution to mesh refinement. Based on the mesh-independence assessment and the need to accurately capture the swirling flow and recirculation structures, the fine mesh was selected for the subsequent simulations. A relative error of less than 5% was observed.

Results and Discussion

The numerical study of ULDW on swirl formation and turbulent modeling is presented below using velocity profiles, pressure distributions, and swirl numbers.

Velocity Profiles

The radial distribution of axial velocity at $z = 60$, 30, and 10 mm is presented in Figure 2. The velocity profiles exhibit a characteristic increase from the central region toward an off-axis maximum, followed by a gradual reduction toward the outer radial region. The maximum axial velocity is approximately 100–112m/s, despite the prescribed inlet velocity of 45 m/s as shown in Figure 2 (b). This local acceleration is associated with the interaction of the four tangentially injected gas jets and the conversion of inlet momentum into a combined axial–circumferential flow. The off-axis maximum indicates that the flow is strongly influenced by the developing vortex rather than behaving as a conventional fully developed axial jet [11].

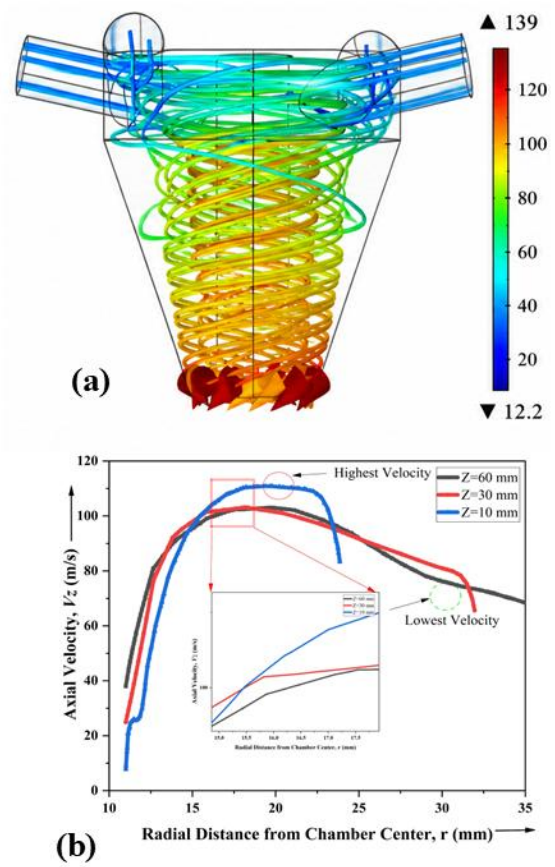


Figure 2. (a) Velocity streamlines, (b) Axial Velocity and its variation at the radial distance (top to bottom)

The profiles at different axial locations also show that the velocity distribution changes progressively along the conical chamber. In the upper region, strong jet interaction produces large velocity gradients, while downstream the flow becomes more evenly distributed across the chamber cross-section. From the perspective of underwater local dry welding, this velocity redistribution is important because it determines how rapidly the supplied gas is transported through the chamber and distributed around the welding region. A sufficiently energetic flow can promote water displacement and continuous gas renewal; however, excessive local velocity may increase turbulence and pressure losses. Thus, the velocity field demonstrates that the chamber geometry and tangential inlet arrangement strongly govern the gas-flow characteristics required for maintaining a stable local dry environment.

Pressure Distribution

The pressure distribution inside the chamber and the corresponding radial pressure profiles are shown in Figure 3.

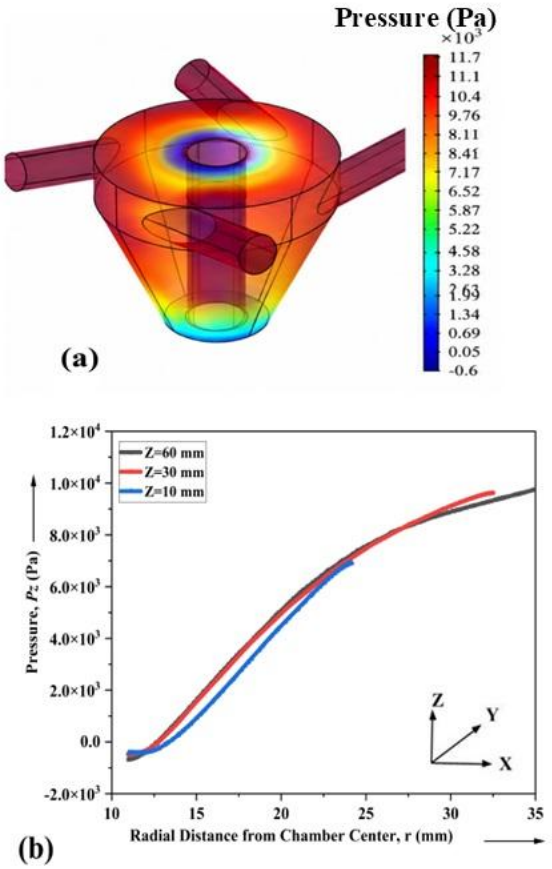


Figure 3. Pressure variation in the chamber (a) surface plot and (b) Line plot showing pressure variation from (top to bottom)

The pressure contour indicates a strongly non-uniform pressure field, with relatively high pressure in the upper chamber region and a progressive

reduction toward the lower conical section and outlet.

The calculated pressure ranges from approximately -0.6 × 10^3 Pa to 11.7 × 10^3 Pa. The radial profiles at Z = 60 mm, 30 mm, and 10 mm show a similar overall trend, with pressure increasing from the inner region toward the outer regions. This radial pressure variation is a characteristic feature of swirling flow because the circumferential velocity produces a radial pressure gradient that balances the centrifugal tendency of the rotating gas [12]. In addition, acceleration, turbulent momentum transfer, wall friction, and the changing cross-sectional geometry contribute to the observed pressure redistribution. The lower pressure near the outlet is also consistent with the prescribed outlet pressure condition of 0 Pa. For underwater local dry welding, the pressure field is particularly important because the gas pressure within the chamber must provide sufficient resistance against surrounding water intrusion while allowing continuous drainage through the outlet. Therefore, chamber performance should be evaluated using the local pressure field rather than the outlet pressure alone. A future water–air multiphase or hydrostatic analysis would be required to quantitatively determine the water-exclusion capability.

Swirl Number

The axial progress of the swirl number at 12 locations along the conical chamber is presented in Figure 4. The swirl number initially decreases sharply from approximately 7.6 at z=1 (60 mm from the top) to 3.10 at z=3 (50 mm from the top), then increases progressively to approximately 6.2 at point 6 (approximately 35 mm from the top). Subsequently, the swirl number decreases continuously and reaches approximately 1.17 at the final location (z = 12 (15 mm above outlet)). The non-monotonic variation indicates that the vortex does not evolve as a simple, continuously decaying rotational flow. Instead, the four tangential inlet jets interact with one another and with the chamber walls, causing redistribution and reorganization of angular momentum along the conical section. The initial reduction is therefore associated with strong jet interaction and momentum redistribution, whereas the subsequent increase indicates redevelopment of coherent circumferential motion within the chamber.

Further downstream, wall interaction, turbulent mixing, and the conversion of circumferential momentum into axial transport progressively reduce the angular-momentum flux, ultimately reducing swirl [13], [14] . The high inlet swirl is beneficial for distributing drainage gas circumferentially around the welding region, potentially improving gas coverage and reducing localized water-entry paths.

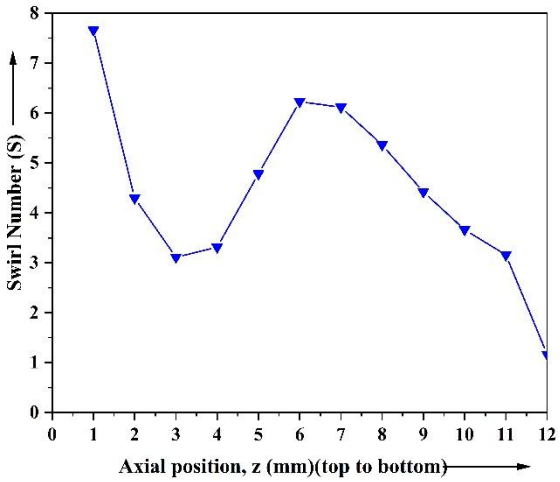


Figure 4. Swirl number distribution over various points on the conical skirt (top to bottom)

However, excessive swirl can also generate strong recirculation and pressure gradients. The downstream reduction toward $S = 1.17$ suggests progressive stabilization of the flow and increased axial transport toward the outlet, providing an important basis in flow physics for optimizing the chamber geometry and inlet configuration for local dry underwater welding.

Conclusions

The present study numerically characterized the three-dimensional swirling gas flow inside a ULDW chamber using COMSOL Multiphysics® 6.3 with the stationary RANS–SST turbulence model. The results demonstrate that the four angled and tangential inlets generate a strong rotational flow accompanied by noteworthy axial velocity gradients, non-uniform pressure distribution, and vortex development within the chamber. The radial velocity profiles confirmed substantial flow acceleration and momentum redistribution, while the pressure field exhibited strong spatial variation associated with swirling motion, flow acceleration, and chamber geometry. Most importantly, the swirl-number analysis revealed a highly non-monotonic vortex evolution, with the swirl number decreasing from approximately 7.66 near the inlet to 1.17 near the outlet, indicating progressive redistribution and dissipation of angular momentum along the conical section. These findings establish that inlet-induced swirl is a governing mechanism controlling gas distribution, pressure characteristics, and flow stabilization. The study therefore provides a quantitative CFD-based foundation for optimizing inlet configuration and flow conditions to improve gas coverage and water-exclusion capability in underwater local dry-welding chambers.

References

[1] A. Vijay and N. Radhika, "A comprehensive review on underwater welding: methods, property evaluations and challenges," *Advances in Materials and Processing Technologies*, vol. 10, no. 2, pp. 923–959, Apr. 2024, doi: 10.1080/2374068X.2023.2184582.

[2] F. Yusof and M. F. Jamaluddin, "Welding Defects and Implications on Welded Assemblies," *Comprehensive Materials Processing: Thirteen Volume Set*, vol. 6, pp. V6-125-V6-134, Jan. 2014, doi: 10.1016/B978-0-08-096532-1.00605-1.

[3] C. Hu *et al.*, "Investigation on microstructure and properties of the local dry underwater TIG welding of 304L stainless steel," *Mater. Today Commun.*, vol. 44, p. 111978, Mar. 2025, doi: 10.1016/J.MTCOMM.2025.111978.

[4] L. Han, X. Wu, G. Chen, Z. Wang, and W. Fan, "Local dry underwater welding of 304 stainless steel based on a microdrain cover," *J. Mater. Process. Technol.*, vol. 268, pp. 47–53, Jun. 2019, doi: 10.1016/J.JMATPROTEC.2018.12.029.

[5] H. Liao *et al.*, "Numerical simulation and experimental verification of droplet transfer during local dry underwater MIG welding process of SUS304," *Journal of Materials Research and Technology*, vol. 21, pp. 1960–1973, Nov. 2022, doi: 10.1016/J.JMRT.2022.10.040.

[6] L. Han, K. Pei, F. Sun, Z. Wang, and Q. Zhang, "Numerical Simulation on the Effect of Gas Pressure on the Formation of Local Dry Underwater Welds," *ISIJ International*, vol. 61, no. 3, pp. 902–910, Mar. 2021, doi: 10.2355/ISIJINTERNATIONAL.ISIJINT-2020-367.

[7] K. U. Bhaskar, Y. R. Murthy, M. R. Raju, S. Tiwari, J. K. Srivastava, and N. Ramakrishnan, "CFD simulation and experimental validation studies on hydrocyclone," *Miner. Eng.*, vol. 20, no. 1, pp. 60–71, Jan. 2007, doi: 10.1016/J.MINENG.2006.04.012.

[8] "COMSOL Documentation." Accessed: Sep. 17, 2026. [Online]. Available: https://doc.comsol.com/6.3/docserver/#!/com.comsol.help.cfd/html_CFDModuleManual.html

[9] "CFD Module User's Guide," 1998. [Online]. Available: www.comsol.com/blogs

[10] Y. Gao, X. Zhang, W. Han, J. Li, and L. Yang, "Effects of swirl number and bluff body on swirling flow dynamics," *AIP Adv.*, vol. 13, no. 2, Feb. 2023, doi: 10.1063/5.0132024/2877633.

[11] A. F. Nowakowski and T. Dyakowski, "Investigation of Swirling Flow Structure in Hydrocyclones," *Chemical Engineering Research and Design*, vol. 81, no. 8, pp. 862–873, Sep. 2003, doi: 10.1205/026387603322482103.

[12] Y. R. Murthy and K. U. Bhaskar, "Parametric CFD studies on hydrocyclone," *Powder Technol.*, vol. 230, pp. 36–47, Nov. 2012, doi: 10.1016/J.POWTEC.2012.06.048.

[13] H. A. H. Sehole, G. Mehdi, R. Riaz, A. Ul Jabbar, A. Maqsood, and M. G. De Giorgi, "Quantifying Swirl Number Effects on Recirculation Zones and Vortex Dynamics in a Dual-Swirl Combustor," *Energies 2025, Vol. 18, Page 6568*, vol. 18, no. 24, p. 6568, Dec. 2025, doi: 10.3390/EN18246568.

[14] G. Vignat, D. Durox, and S. Candel, "The suitability of different swirl number definitions for describing swirl flows: Accurate, common and (over-) simplified formulations," *Prog. Energy Combust. Sci.*, vol. 89, p. 100969, Mar. 2022, doi: 10.1016/J.PECS.2021.100969.

Acknowledgements

The authors want to thank the National Institute of Technology, Mizoram, for their firm support throughout the research and development. One of the authors, Dr. Saurav Suman, gratefully acknowledges the seed grant supporting this work. Authors are grateful for the financial support for this study from the Indian Institute of Technology Guwahati, Technology Innovation Hub (TIH) under DST, Govt. of India (Grant No: TIH project (TIH/TD/0107)).